Journal of Power Sources 196 (2011) 1012–1018

Contents lists available at ScienceDirect

Journal of Power Sources

journal homepage: www.elsevier.com/locate/jpowsour

# Preparation and characterization of Pt supported on graphene with enhanced electrocatalytic activity in fuel cell

Yuchen Xin[a,b], Jian-guo Liu[a,b,*], Yong Zhou[a], Wenming Liu[a], Jian Gao[b], Yun Xie[b], Ying Yin[b], Zhigang Zou[a,**]

[a] Eco-materials and Renewable Energy Research Center, Department of Physics and National Laboratory of Solid State Microstructures, Nanjing University, Nanjing 210093 China
[b] Department of Materials Science and Engineering, Nanjing University, Nanjing 210093 China

ARTICLE INFO

*Article history:*
Received 6 July 2010
Received in revised form 18 August 2010
Accepted 18 August 2010
Available online 26 August 2010

*Keywords:*
Fuel cell
Graphene
Platinum supported on graphene
Heat treatment

ABSTRACT

Pt nanoparticles are deposited onto graphene sheets via synchronous reduction of $H_2PtCl_6$ and graphene oxide (GO) suspension using $NaBH_4$. Lyophilization is introduced to avoid irreversible aggregation of graphene (G) sheets, which happens during conventional drying process. Pt/G catalysts reveal a high catalytic activity for both methanol oxidation and oxygen reduction reaction compared to Pt supported on carbon black (Pt/C). The performance of Pt/G catalysts is further improved after heat treatment in $N_2$ atmosphere at 300 °C for 2 h, and the peak current density of methanol oxidation for Pt/G after heat treatment is almost 3.5 times higher than Pt/C. Transmission electron microscope (TEM) images show that the Pt particles are uniformly distributed on graphene sheets. X-ray photoelectron spectroscopy (XPS) results demonstrate that the interaction between Pt and graphene is enhanced during annealing. It suggests that graphene has provided a new way to improve electrocatalytic activity of catalyst for fuel cell.



## 1. Introduction

Direct methanol fuel cells (DMFC) have drawn great attention recently due to its high energy density, low pollutant emission, low operating temperature (60–100 °C), and ease of handling liquid fuel [1]. However, the low electrocatalytic activity of methanol oxidation is still obstacle inhibiting broad application of DMFC.

Carbon black (Vulcan XC-72, Cabot Crop.), is widely used as supporting material for Pt (Pt/C) because of its high surface area and low cost. However, the insufficient performance of Pt/C as well as long term stability of carbon black under fuel cell operation still calls for new and improved materials. Recently, carbons with different structures such as nanotubes (CNTs) and nanofiblers (CNFs) have been studied extensively as electrocatalysts supports, due to their unique electric and micro- and macrostructure properties [2–7]. Since the single-layer graphene was discovered first in 2005 [8–10], it has attracted great interest from both the experimental and theoretical scientific communities [11].

Graphene exhibits the structure of two-dimensional sheet composed of $sp^2$-bonded carbon atoms, and has unique physical properties such as high surface areas (theoretical specific surface area of 2620 $m^2\,g^{-1}$), superior electric conductivities and excellent mechanical strength and elasticity. Therefore, graphene may provide a new way to improve electrocatalytic activity of catalyst in fuel cell [7,12]. However, there are still some critical problems for the investigation of graphene as catalysts support. For example, the reduced graphene sheets tend to form irreversible agglomerates because of the van der Waals interaction and even restack to form graphite in the reduction from GO suspension solution or drying process [13]. The aggregation of graphene sheets will not only ruin the advantage of high surface area of graphene, but also obstruct the dispersion of Pt/G in the catalyst ink.

In this study, Pt/G was simply prepared by synchronous reduction of $H_2PtCl_6$ and graphene oxide (GO). Lyophilization was first used to prevent irreversible aggregation of graphene sheets during drying process and heat treatment was introduced to improve the electrochemical characteristics of Pt/G catalysts. TEM and XPS were employed to characterize morphology and surface composition of all samples. The catalytic activity of Pt/G showed better performance than that of Pt/C for methanol oxidation and oxygen reduction reaction. Furthermore, the performance of Pt/G was

* Corresponding author at: ERERC, Department of Materials Science and Engineering, Nanjing University, 22 Hankou Road, Nanjing 210093, China. Tel.: +86 25 83621219; fax: +86 25 83686632.
** Corresponding author at: ERERC, Department of Physics, Nanjing University, 22 Hankou Road, Nanjing 210093, China. Tel.: +86 25 83686630.
*E-mail addresses:* jianguoliu@nju.edu.cn (J.-g. Liu), zgzou@nju.edu.cn (Z. Zou).

0378-7753/$ – see front matter © 2010 Elsevier B.V. All rights reserved.
doi:10.1016/j.jpowsour.2010.08.051

enhanced after heat treatment. It suggests that graphene is a promising supporting material for noble metal catalysts in DMFC.

## 2. Experimental

### 2.1. Sample preparation

The graphene oxide (GO) was synthesized from natural graphite powder by a modification of Hummers and Offenman's method [14,15]. In brief, 2 g of graphite, 2 g of $NaNO_3$, and 92 ml of concentrated $H_2SO_4$ were stirred together in an ice bath. Then 12 g of $KMnO_4$ was slowly added into it. The solution was then stirred at $35 \pm 5\,^{\circ}C$ for 1 h. Pure water with a volume of 160 ml was added and the temperature was kept at $90 \pm 5\,^{\circ}C$ for 30 min. Finally, 400 ml of pure water and 12 ml of $H_2O_2$ (30%) was put into the mixture. The solution was filtered and the filter cake was dispersed in water by ultra-sonic bath. The mixture was washed with 1:10 HCl solution and water by repeated centrifugation. The obtained sediment was dispersed in water with the help of ultra-sonic bath and dried in air at 45 °C overnight. The graphene oxide with a weight of 90 mg was dispersed in 20 ml $H_2O$ by sonication for 30 min before 1.35 ml $H_2PtCl_6$ solution (20 mg $H_2PtCl_6{\cdot}6H_2O$ $ml^{-1}$) was added. The pH value of this mixture was adjusted to 10 using ammonia, which could partly protect carboxylic acid groups. Excessive $NaBH_4$ aqueous solution with a concentration of 2 mg $ml^{-1}$ was slowly added and stirred for 12 h under room temperature. The solution was filtered via vacuum filtration using buchner funnel and further washed with hot water. The residue was re-dispersed in water by sonication and dried by lyophilization, which can prevent irreversible aggregation of graphene during drying process.

Moreover, Pt/G catalyst was annealed at 300 °C in $N_2$ atmosphere for 2 h, which was denoted as Pt/G-A. Pt supported on carbon (Vulcan XC-72, Cabot Corp.) was also synthesized by the same method for comparison. Pt loading in all samples was kept the same as 10 wt%.

### 2.2. Physical and electrochemical characterizations

The X-ray diffraction (XRD) was conducted on a Rigaku D/MAX-Ultima III X-ray diffractometer using Cu Kα radiation ($\lambda = 0.15406$ nm). The $2\theta$ angular ranges from 10° to 80° were explored at a scan rate of 10° $min^{-1}$. The X-ray photoelectron spectroscopy (XPS) was performed by ESCALAB 250 apparatus, using monochromated Al Kα radiation at 150 W, in the pass energy (PE) mode (PE = 20 eV). All of the spectra were obtained under identical conditions. The pressure of the spectrometer was $5 \times 10^{-10}$ and $5 \times 10^{-9}$ mbar during the measurements. The morphology of Pt nanoparticles on different carbon supports was explored by transmission electron microscope (TEM) on a JEM-200CX at 200 kV and scanning electron microscope (SEM) on a FEI NOVA NanoSEM 230 at 15 kV.

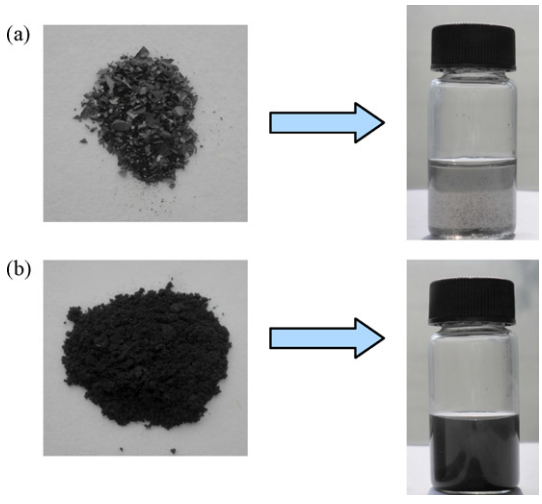


**Fig. 1.** Graphene supported platinum powder and suspension in water (1 mg $ml^{-1}$). (a) Pt/G by conventional drying and (b) Pt/G by lyophilization drying.

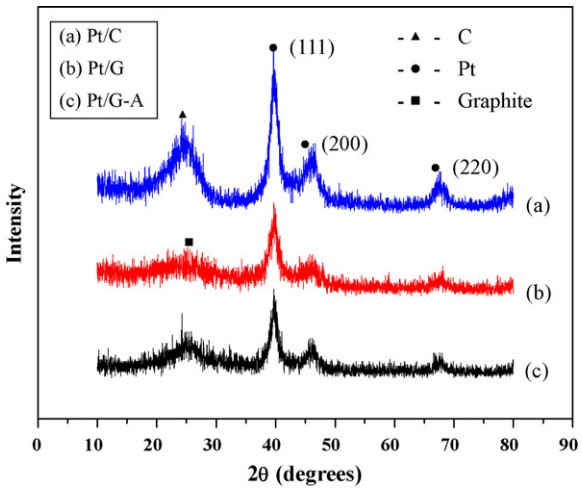


**Fig. 2.** XRD patterns of (a) Pt/C, (b) Pt/G, and (c) Pt/G-A.

Electrochemical measurements were conducted at a three-electrode cell using PARSTAT 2273 workstation (Princeton Applied Research). Pt foil was served as a counter electrode while saturated calomel electrode (SCE) was used as a reference electrode and glass carbon disk with a diamond of 5 mm as a working electrode. Catalyst powder with a weight of 5 mg was dispersed in 100 μl of 5% Nafion and 900 μl of ethanol solution and sonicated for 30 min. Then 10 μl of the slurry was dropped onto the surface of a glassy carbon electrode with an area of 0.196 $cm^2$ to form a thin layer. The total Pt loading on the working electrode was 5 μg for all Pt catalysts. For cyclic voltammetry (CV) measurements, the working electrode was immersed in 0.5 M $H_2SO_4$ in 0.5 M $CH_3OH$ solution saturated by high purified nitrogen with the potential between −0.241 and 1.0 V versus SCE. Before the oxygen reduction experiment, the solution was purged with 99.999% $O_2$ for at least 20 min. The scanning potential was from 1.0 to 0 V versus SCE with a scan rate of 5 mV $s^{-1}$. All potentials were measured and quoted against the saturated calomel electrode (SCE).

## 3. Results and discussion

Pt supported on graphene was successfully synthesized by the synchronous reduction of $H_2PtCl_6$ and graphene oxide (GO) suspension using $NaBH_4$ as shown in Fig. 1. The suspended substance became black from initial brown color and precipitated once $NaBH_4$ was added. The final appearance of Pt/G powder seriously depends on the drying process. As showed in Fig. 1a, Pt/G tended to form a stack of graphitic structure when the suspension was dried by conventional evaporation of water in the suspension. Si et al. [16] reported that Pt can act as spacers for graphenes and lead to a potential high-surface-area material. However, the aggregation of Pt/G was still severe according to our experiments if it was dried by conventional method. Most of important, the redispersion of Pt/G in water or alcohol became impossible even under the help of high power sonication once it was aggregated during dehydration as showed in Fig. 1a. Catalyst ink is almost necessary when making fuel cell electrodes whether by casting, screen-printing or spraying method. Therefore, great efforts have been devoted to disperse

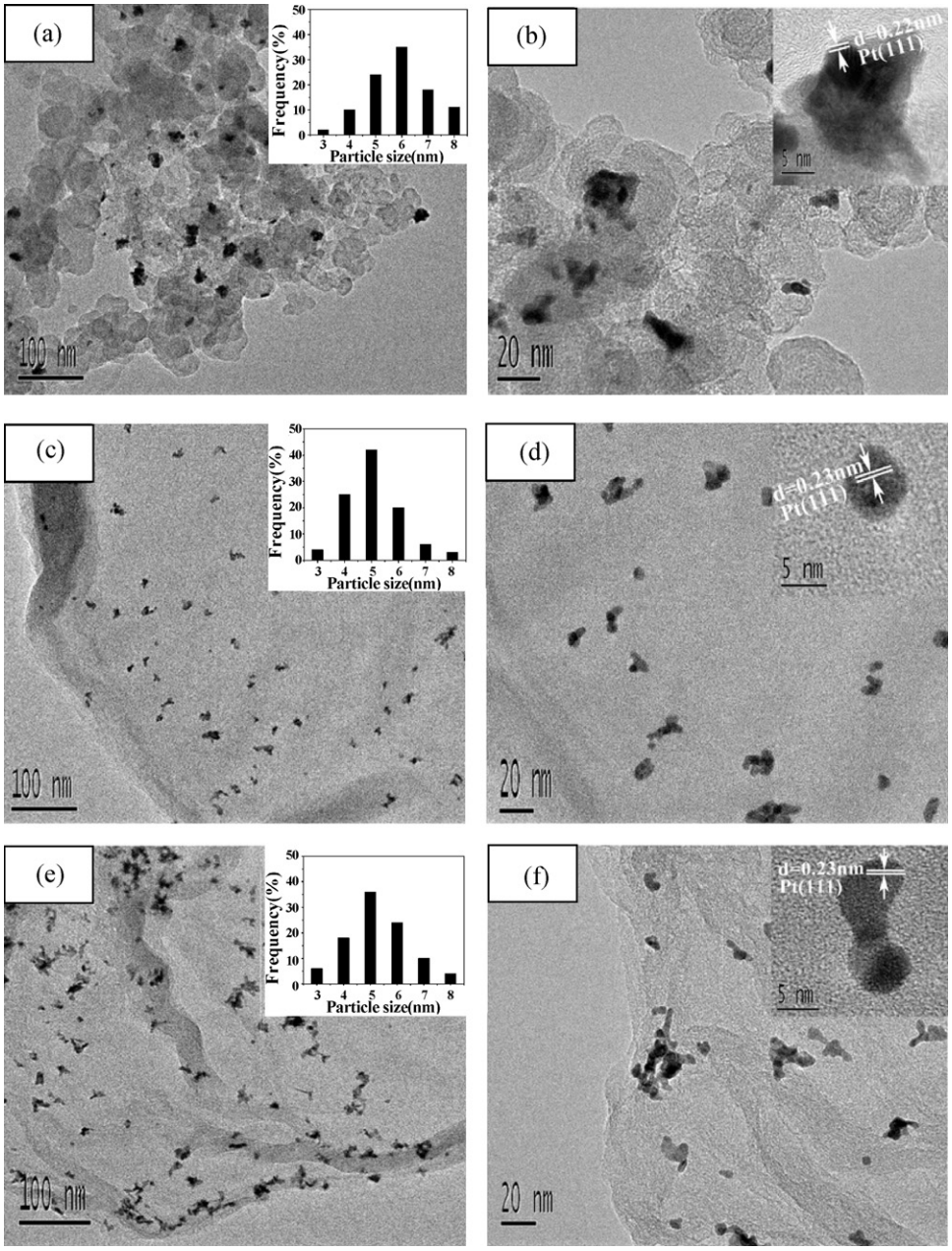


**Fig. 3.** TEM images and histogram of Pt particles of (a and b) Pt/C, (c and d) Pt/G and (e and f) Pt/G-A.

graphene sheets in water or other solvents by adding surfactant or functionalizing the surface of graphene. However, these surfactants are unfriendly to Pt catalysis in fuel cell and also can result in poor electronic conductance as well [17]. In this study, lyophilization was introduced to prevent the restack of these sheets during liquid water departure in the conventional drying process. The water in the suspension can be sublimated from solid ice to gas, which can prevent accumulation of Pt/G. It can be seen from Fig. 1b that porous Pt/G in the dry state can be obtained when using lyophilization. Moreover, the isolated Pt/G sheets can be re-dispersed in water without any difficulty. It indicated that lyophilization was a facile and efficient approach to produce Pt/G ink. On the other hand, more Pt particles in such isolated structure would be exposed to electrolyte solution, thus lead to higher catalytic performance.

Fig. 2 showed the XRD patterns of 10 wt% Pt/C, Pt/G and Pt/G-A catalysts. The diffraction peaks at 39.8°, 46.3°, and 67.5° can be indexed to the (1 1 1), (2 0 0), and (2 2 0) planes of the face-centered cubic (fcc) phase of Pt [18], while those at 26.5° corresponding to graphite [12]. From the full width half maximum of the (2 2 0) peak, the volume-averaged particles size was calculated from the Scherrer equation [19]. The average Pt particle sizes were 6, 5 and 5 nm for Pt/C, Pt/G and Pt/G-A, respectively, suggesting larger Pt specific surface area in graphene. The size of Pt particles supported on graphene was a little bit small, which indicated that unique structure and physical properties of graphene can be helpful for the distribution of Pt nanoparticles. Furthermore, no significant phase changes were observed for Pt/G after heat treatment at 300 °C in $N_2$.

The morphology, the size, and the dispersion of Pt catalysts were examined by TEM. It can be found from Fig. 3 that Pt particles with the average particle size of 5.7 nm deposited on XC-72 carbon black aggregated seriously, while the “Pt nano clusters” were uniformly distributed on graphene sheets. The “Pt nano clusters” consisted of small particles with diameter ranging from 3 to 8 nm in Fig. 3d

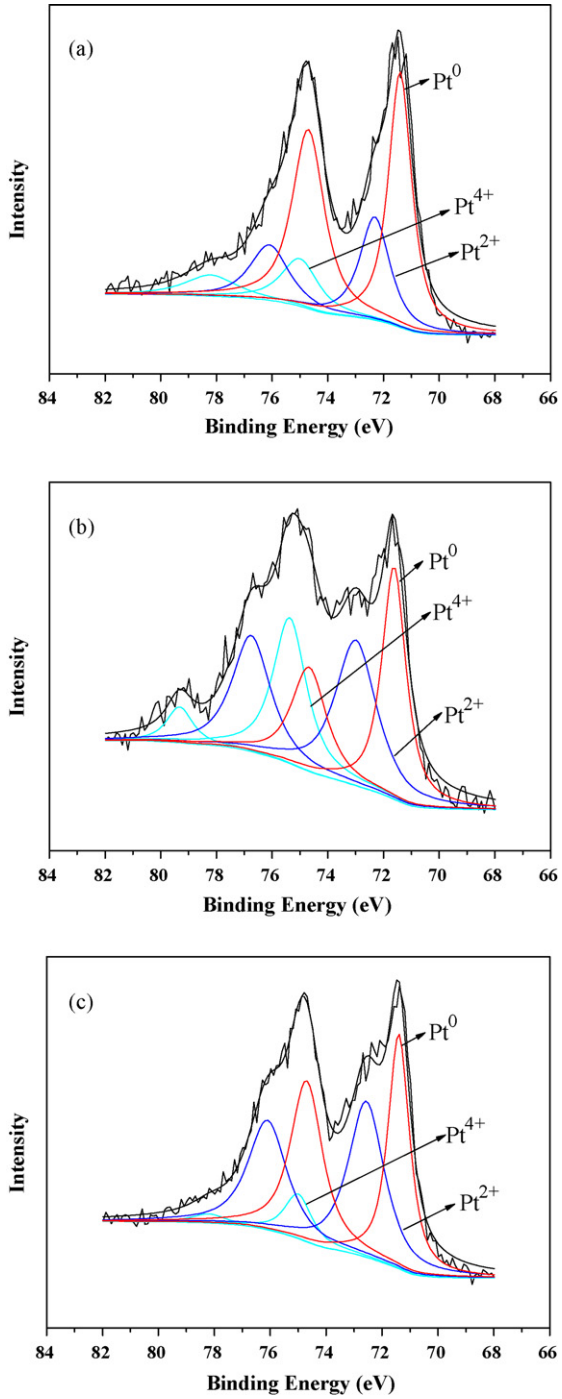


**Fig. 4.** Pt(4f) XPS spectra of (a) Pt/C, (b) Pt/G and (c) Pt/G-A.

and e. The size distributions were obtained by measuring the sizes of 100 randomly selected particles. The average particle size was 5.1 nm for Pt/G and 5.2 nm for Pt/G-A, indicating that the Pt aggregation was not serious after annealing. The stability of Pt particles on the surface of graphene after heat treatment suggested that there might be a relatively strong interaction between graphene and Pt particles [7]. The interaction between graphene and Pt may influence the electronic structure of Pt, and also possibly improve the performance of catalysts. The high resolution TEM images showed that the space of lattice fringes were 0.22–0.23 nm, which was corresponding with (1 1 1) planes of Pt.

**Table 1**
Relative intensity values for different Pt species as observed from Pt(4f) spectra for different catalysts.

| Catalyst | Pt species | Relative intensity (%) |
|---|---|---|
| Pt/C | $Pt^0$ | 59.3 |
| | $Pt^{2+}$ | 26.3 |
| | $Pt^{4+}$ | 14.4 |
| Pt/G | $Pt^0$ | 36.3 |
| | $Pt^{2+}$ | 40.9 |
| | $Pt^{4+}$ | 22.8 |
| Pt/G-A | $Pt^0$ | 47.6 |
| | $Pt^{2+}$ | 45.4 |
| | $Pt^{4+}$ | 7.0 |

Fig. 4 showed the Pt(4f) X-ray photoemission spectroscopy (XPS) results for all catalysts. The principle peaks were attributed to $Pt^0$ at 71.4 eV ($4f_{7/2}$) and 74.7 eV ($4f_{5/2}$), while 72.8, 76.1 and 75.0, 78.2 eV were assigned to Pt in 2+ and 4+ states, respectively [20]. The results of different Pt species were calculated based on above data and listed in Table 1. The relative intensity of $Pt^0$, $Pt^{2+}$ and $Pt^{4+}$ was calculated to be 36.3, 40.9 and 22.8% for Pt/G catalyst, respectively. After heat treatment, the proportion of $Pt^0$ on the surface increased to 47.6%, while $Pt^{4+}$ decreased to 7%. It indicated that the $PtO_x$ had been mostly reduced to metallic Pt.

The XPS spectrum of C(1s) was also shown in Fig. 5. Different functional groups were presented in samples: the non-oxygenated ring C (C–C, 284.6 eV), the C in C–O bond (C–O, 286.6 eV) and the carbonyl C (C=O, 288.5 eV) [21]. The relative intensity of the different carbon species obtained from the respective area was also listed in Table 2, which shows that heat treatment changed car-

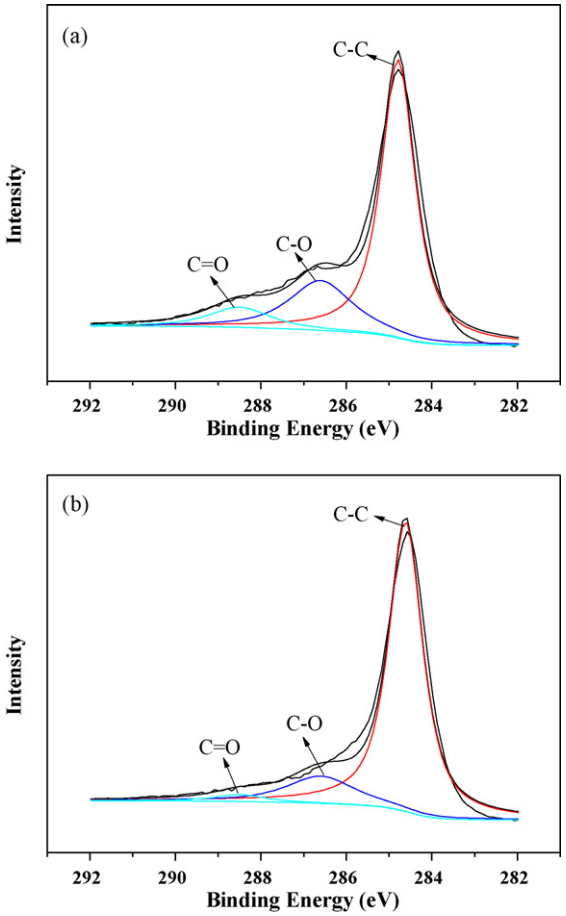


**Fig. 5.** C(1s) XPS spectra of (a) Pt/G and (b) Pt/G-A.

**Table 2**
Relative intensity values for different components as observed from C(1s) spectra for different catalysts.

| Catalyst | C species | Relative intensity (%) |
|---|---|---|
| Pt/G | C–C | 68.4 |
| | C–O | 22.7 |
| | C=O | 8.9 |
| Pt/G-A | C–C | 81.8 |
| | C–O | 15.4 |
| | C=O | 2.8 |

bon surface functional groups graphene primarily by reducing the amount of oxygen-containing species. The relative intensity of C–O and C=O decreased dramatically during annealing. It implied that the functional groups such as carboxyl groups, hydroxyl groups, and epoxy groups [22] were oxidized and detached from graphene surface during heat treatment. In addition, PtO and $PtO_2$ in Pt/G can be reduced in the presence of functional groups under heat treatment. Therefore, the interaction between Pt and graphene was further enhanced.

Fig. 6 illustrated the cyclic voltammetry (CV) curves of different samples in nitrogen saturated 0.5 M $H_2SO_4$ solution with a potential range from −0.241 to 1.0 V versus SCE. The CV profiles of platinum supported on graphene with or without heat treatment were quite different to those of Pt supported on carbon black (XC-72). Current peaks around 0.4 V in the forward scan and 0.3 V in the backward scan were clearly observed for samples containing graphene. It can be noticed that CV curve of graphene (Fig. 6e) under the same experimental condition can also show similar profile like Pt/G and Pt/G-A. Therefore, samples with the irregular current peaks were possibly caused by graphene, which contain oxygen-containing groups such

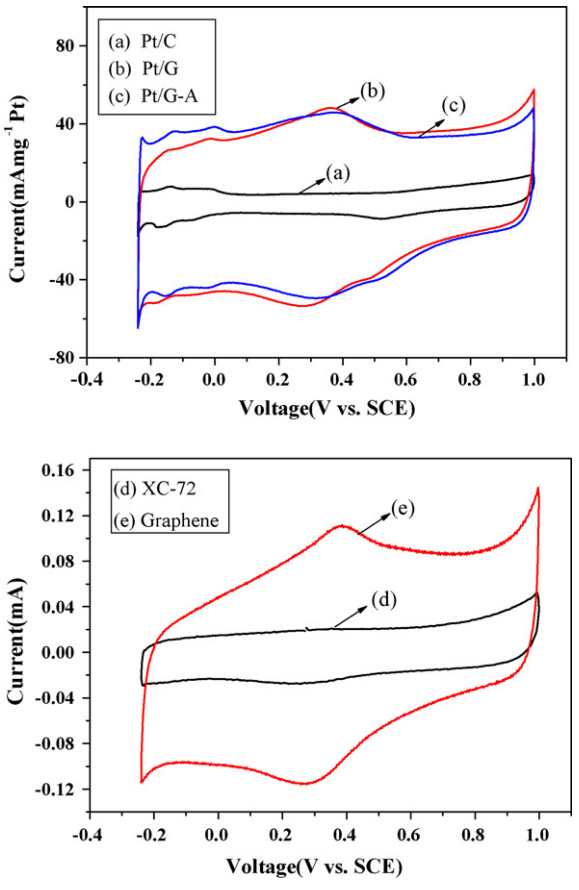


**Fig. 6.** Cyclic voltammograms of (a) Pt/C, (b) Pt/G, (c) Pt/G-A, (d) XC-72 and (e) Graphene. Scan rate = 20 mV $s^{-1}$ at room temperature in 0.5 M $H_2SO_4$.

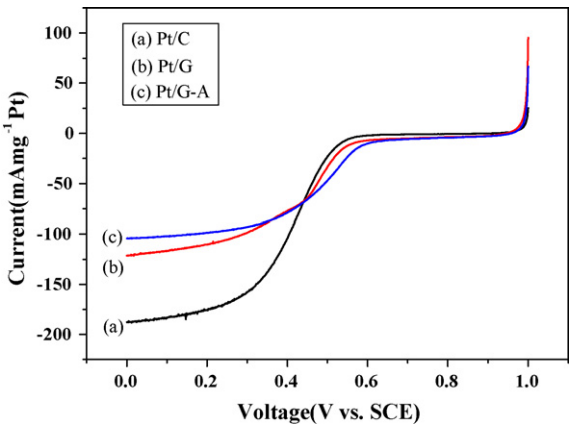


**Fig. 7.** Polarization curves for ORR on (a) Pt/C, (b) Pt/G and (c) Pt/G-A. $O_2$-saturated 0.5 M $H_2SO_4$ solution, scan rate: 5 mV $s^{-1}$, rotation rate: 2500 rpm.

as carboxyl groups, hydroxyl groups, and epoxy groups from the results of XPS in Fig. 5. The electrochemically active surface area (ECSA) provided important information regarding the number of available active sites, which was estimated by hydrogen adsorption/desorption from the electrode surface [23]. As shown in Fig. 6, ECSAs for those catalysts were hard to estimate due to the disturbing of the "oxygen-containing peaks" around 0.4 and 0.3 V. However, ECSAs of Pt/G and Pt/G-A should be higher because its currents in −0.19 to 0.16 V range were much higher than Pt/C.

Fig. 7 showed the oxygen reduction reaction (ORR) measurements in an $O_2$-saturated 0.5 M $H_2SO_4$ solution. The onset potential of Pt/G-A showed a 40 mV shift to positive one compared with Pt/C and Pt/G. The electrochemical reaction seemed to be under kinetic and diffusion control in the range of 0.63–0.2 V and the diffusion-limiting currents were obtained in the potential region below 0.2 V. Pt/G and Pt/G-A showed a smaller limiting current in ORR than that of Pt/C. It was believed that the diffusion-limiting currents were strongly affected by the structure of the catalyst supporting material. The sheet structure of graphene might block oxygen diffusion a little bit compared with spherical carbon black particles. The half wave potential (defined as the potential at which the measured current reached the half of the limiting current) was 404, 461 and 495 mV for Pt/C, Pt/G and Pt/G-A respectively, which showed an increase in the activity with the enhancement of the half wave potential [24]. This was also accordance with the trend observed for CV results in Fig. 6.

The activity of methanol electro-oxidation of three samples in the solution of 0.5 M $CH_3OH$ and 0.5 M $H_2SO_4$ was shown in Fig. 8. The onset potential of methanol oxidation was about 0.4 V, and the anodic current peak was around 0.61 V. The peak current density of Pt/G catalysts was 182.6 mA $mg^{-1}$ Pt while that of Pt/C catalysts was only 77.9 mA $mg^{-1}$ Pt. Furthermore, it raised to 261.6 mA $mg^{-1}$ Pt for Pt supported on graphene after heat treatment, which showed a higher catalytic than the performance reported by previous literature [25] (the peak current density is 199.6 mA $mg^{-1}$ Pt). The enhanced catalytic activity may be due to the unique interaction between Pt and graphene. Pt supported on graphene can exhibit larger ECSA, which can offer more Pt activity sites for chemisorption of methanol.

Ye et al. [26] and Liu et al. [27] also reported that heat treatment can increase activity of catalysts. This behavior can be explained by the morphology modification of support, Pt dispersion and Pt crystallite growth on the supports. The surface of graphene is very heterogeneous and contains a wide variety of functional groups, which can significantly affect the chemical properties. Regarding Pt deposition on graphene, the decomposition and redistribution of surface oxygen-containing groups during heat treatment can affect

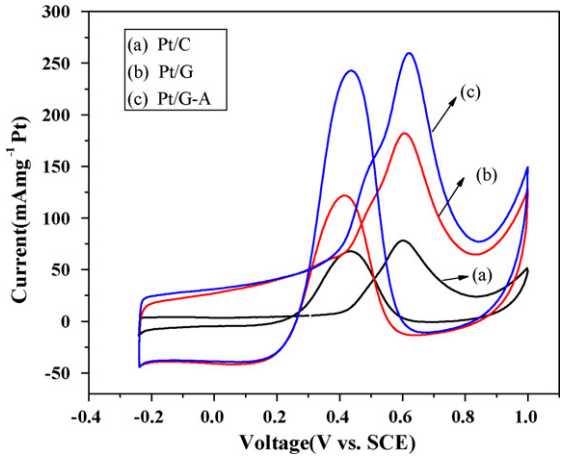


**Fig. 8.** Cyclic voltammograms of methanol oxidation on (a) Pt/C, (b) Pt/G, and (c) Pt/G-A. Scan rate: 20 mV $s^{-1}$, 0.5 M $H_2SO_4$ and 0.5 M $CH_3OH$.

the dispersion and growth of Pt crystallites. Moreover, heat treatment can change Pt surface morphology from amorphous to more ordered states, introducing more active catalytic sites [28].

The stability of the catalysts was examined by chronoamperometry for methanol oxidation in 0.5 M $H_2SO_4$ + 0.5 M $CH_3OH$ at 0.6 V versus SCE. As seen from Fig. 9, the current density of all catalysts decayed rapidly at the initial stage, which might be due to the formation of intermediate species during methanol oxidation such as $CO_{ads}$ and $CHO_{ads}$ [25,29]. The current gradually reached a steady state after quick decayed at the beginning. The Pt/G-A showed the best activity and stability with the ending current of 55.5 mA $mg^{-1}$ Pt after 1200 s. The stability of the catalysts also followed the order of Pt/G-A > Pt/G > Pt/C, which was the same trend for the cyclic voltammetry and methanol oxidation results.

It was well known that GO can form well-dispersed collides because of the electrostatic repulsion between the oxygen-containing functional groups [30,31]. These groups could provide binding sites for anchoring precursor metal ions or metal nanoparticles [32]. Pt particles therefore can easily deposit on graphene when reducing agent was introduced. The particles attached onto graphene sheets also obstruct the formation of a stacked graphitic structure. Additionally, lyophilization can prevent graphene sheets and Pt particles aggregation effectively during the preparation. On the other hand, graphene prepared by chemical reduction may involve some chemical and physical defects due to the introduction of these functional groups. Graphene sheets with these defects are easy to be oxidized and are unstable under fuel cell operation [33].

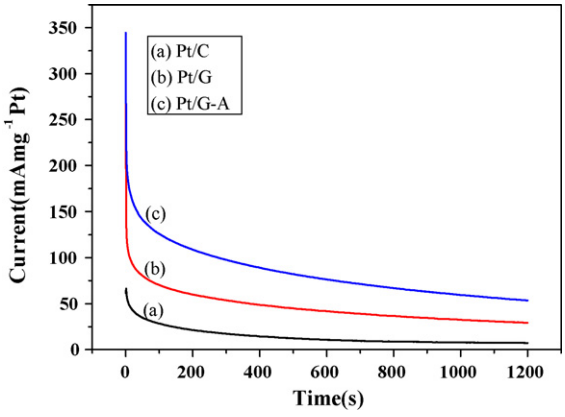


**Fig. 9.** Chronoamperometric curves of methanol electro-oxidation on (a) Pt/C, (b) Pt/G and (c) Pt/G-A. 0.5 M $H_2SO_4$ and 0.5 M $CH_3OH$, potential: 0.6 V versus SCE.

Heat treatment can repair these defects by decomposing partially these functional groups and lead to a decrease in the graphene resistance [34], which improves the stability of graphene. In addition, the curly graphene sheets might roll or break into smaller sheets by thermal tension in the process of annealing [35]. The Pt/G-A may expose more Pt active sites for methanol oxidation. Heat treatment therefore is favorable for the improvement of the electrocatalytic reaction of Pt/G.

## 4. Conclusions

A simply way to synthesize well-dispersed Pt/G catalysts using graphene oxide (GO) as a precursor was demonstrated in this paper. The introduction of lyophilization offered a facile and efficient approach to produce well soluble graphene and heat treatment was employed to improve the performance of Pt/G catalysts. Electrochemical experiments toward methanol oxidation indicated that Pt/G had higher catalytic activity than that of Pt/C, and the stability of Pt/G was better than Pt/C catalysts. Pt/G after heat treatment at 300 °C performed higher intrinsic activity and stability for methanol oxidation, which may be attributed to four effects induced by heat treatment: (1) the enhancement of interaction between Pt and graphene; (2) the additional Pt active sites were exposed by the rolling of grahene sheets; (3) decomposing partially surface functional groups resulted in less defects on graphene, improving the stability of graphene and (4) Pt surface morphology from amorphous to more ordered states, introducing more active catalytic sites. The SEM and TEM results also showed that graphene was in favor of improving the distribution of Pt particles. It indicates that graphene is a promising supporting material to modify catalytic properties of Pt for fuel cell catalysts.

## Acknowledgments

The authors acknowledge the financial support by National Basic Research Program of China (2007CB613300), Natural Science Foundation of China (20906045), Natural Science Foundation of Jiangsu Province of China (BK2008251) and Doctoral Funding (20090091120033) and Scientific Research Foundation for Returned Scholars of Ministry of Education of China.

## References

[1] L.F. Dong, R.R.S. Gari, Z. Li, M.M. Graig, S.F. Hou, Carbon 48 (2010) 781–787.
[2] T. Matsumoto, T. Komatsu, K. Arai, T. Yamazaki, M. Kijima, H. Shimizu, Y. Takasawa, J. Nakamura, Chem. Commun. 7 (2004) 840–841.
[3] T. Matsumoto, T. Komatsu, H. Nakano, K. Arai, Y. Nagashima, T. Yamazaki, M. Kijima, H. Shimizu, Y. Takasawa, J. Nakamura, Catal. Today 90 (2004) 277–281.
[4] E.J. Yoo, T. Okada, T. Kizuka, J. Nakamura, J. Power Sources 180 (2008) 221–226.
[5] J. Prabhuram, T.S. Zhao, Z.K. Tang, R. Chen, Z.X. Liang, J. Phys. Chem. B 110 (2006) 5245–5252.
[6] S. Liao, K.-A. Holmes, H. Tsaprailis, V.I. Briss, J. Am. Chem. Soc. 128 (2006) 3504–3505.
[7] E.J. Yoo, T. Okada, T. Kizuka, M. Kohyama, J. Nakamura, I. Honma, Nano Lett. 9 (2009) 2255–2259.
[8] K.S. Novoselov, A.K. Geim, S.V. Morozov, D. Jiang, Y. Zhang, S.V. Dubonos, I.V. Grigorieva, A.A. Firsov, Science 306 (2004) 666–669.
[9] K.S. Novoselov, A.K. Geim, S.V. Morozov, D. Jiang, M.I. Katsnelson, I.V. Grigorieva, S.V. Dubonos, A.A. Firsov, Nature 438 (2005) 197–200.
[10] Y.B. Zhang, Y.W. Tan, H.L. Stormer, P. Kim, Nature 438 (2005) 201–204.
[11] A.K. Geim, K.S. Novoselov, Nat. Mater. 6 (2007) 183–191.
[12] B. Seger, P.V. Kamat, J. Phys. Chem. C 113 (2009) 7990–7995.
[13] X. Chao, X. Wang, J.W. Zhu, J. Phys. Chem. C 112 (2008) 19841–19845.
[14] W.S. Hummers, R.E. Offenman, J. Am. Chem. Soc. 80 (1958) 1339.
[15] L.J. Cote, K. Franklin, J.X. Huang, J. Am. Chem. Soc. 131 (2009) 1043–1049.
[16] Y.C. Si, E.T. Samulski, Chem. Mater. 20 (2008) 6792–6797.
[17] Y.Y. Liang, D.Q. Wu, X.L. Feng, K. Mullen, Adv. Mater. 21 (2009) 1679–1683.
[18] X.W. Teng, H. Yang, J. Am. Chem. Soc. 125 (2003) 14559–14563.
[19] W. Li, W.J. Zhou, H.Q. Li, Z.H. Zhou, B. Zhou, G.Q. Sun, X. Qin, Electrochim. Acta 49 (2004) 1045–1055.
[20] P. Bera, K.R. Priolkar, A. Gayen, P.R. Sarode, M.S. Hegde, S. Emura, R. Kumashiro, V. Jayaram, G.N. Subbanna, Chem. Mater. 15 (2003) 2049–2060.

[21] C.Y. Su, Y.P. Xu, W.J. Zhang, J.W. Zhao, X.H. Tang, C.H. Tsai, L.J. Li, Chem. Mater. 21 (2009) 5674–5688.
[22] Q.L. Du, M.B. Zheng, L.F. Zhang, Y.G. Wang, J.H. Chen, L.P. Xue, W.J. Dai, G.B. Ji, J.M. Cao, Electrochim. Acta 55 (2010) 3897–3903.
[23] A. Pozio, M.D. Francesco, A. Cemmi, F. Cardellini, L. Giorgi, J. Power Sources 105 (2002) 13–19.
[24] X. Wang, W.Z. Li, Z.W. Chen, M. Waje, Y.S. Yan, J. Power Sources 158 (2006) 154–159.
[25] Y.M. Li, L.H. Tang, J.H. Li, Chem. Commun. 11 (2009) 846–849.
[26] J.L. Ye, J.G. Liu, Z.G. Zou, G. Jun, T. Yu, J. Power Sources 195 (2010) 2633–2637.
[27] Z.F. Liu, M. Mohamand, E.T. Ada, W.M. Reichert, D.E. Nikles, J. Power Sources 164 (2007) 472–480.
[28] C.W.B. Bezerra, L. Zhang, H.S. Liu, K.C. Lee, A.L.B. Marques, E.P. Marques, H.J. Wang, J.J. Zhang, J. Power Sources 173 (2007) 891–908.
[29] A. Kabbabi, R. Faure, R. Durand, B. Beden, J.M. Leger, C. Lamy, J. Electroanal. Chem. 444 (1998) 41–53.
[30] M.I. Katsnelson, K.S. Novoselov, A.K. Geim, Nat. Phys. 2 (2006) 620–625.
[31] S. Stankovich, R.D. Piner, X.Q. Chen, N.Q. Wu, S.T. Nguyen, R.S. Ruoff, J. Mater. Chem. 16 (2006) 155–158.
[32] Y.L. Hsin, K.C. Hwang, C.T. Yeh, J. Am. Chem. Soc. 129 (2007) 9999–10010.
[33] Y.Y. Shao, S. Zhang, C.M. Wang, Z.M. Niea, J. Liu, Y. Wang, Y.H. Lin, J. Power Sources 195 (2010) 4600–4605.
[34] G. Eda, G. Fanchini, M. Chhowalla, Nat. Nanotechnol. 3 (2008) 270–274.
[35] R.D. Heidenreich, W.M. Hess, L.L. Ban, J. Appl. Crystallogr. 1 (1968) 1–8.